



HAL
open science

Integration of optimized low-pass filters in a bandpass filter for out-of-band improvement

Cédric Quendo, Eric Rius, Christian Person, Michel Ney

► **To cite this version:**

Cédric Quendo, Eric Rius, Christian Person, Michel Ney. Integration of optimized low-pass filters in a bandpass filter for out-of-band improvement. *IEEE Transactions on Microwave Theory and Techniques*, 2001, 49 (12), pp.2376-2383. 10.1109/22.971624 . hal-02399520

HAL Id: hal-02399520

<https://hal.science/hal-02399520>

Submitted on 8 Apr 2022

HAL is a multi-disciplinary open access archive for the deposit and dissemination of scientific research documents, whether they are published or not. The documents may come from teaching and research institutions in France or abroad, or from public or private research centers.

L'archive ouverte pluridisciplinaire **HAL**, est destinée au dépôt et à la diffusion de documents scientifiques de niveau recherche, publiés ou non, émanant des établissements d'enseignement et de recherche français ou étrangers, des laboratoires publics ou privés.



Distributed under a Creative Commons Attribution - NonCommercial 4.0 International License

Integration of Optimized Low-Pass Filters in a Bandpass Filter for Out-of-Band Improvement

Cédric Quendo, Eric Rius, Christian Person, and Michel Ney

Abstract—In this paper, we discuss the control and suppression of spurious resonances commonly encountered with distributed bandpass filters. The basic idea consists of introducing low-pass structures within bandpass topologies. By adjusting low-pass filter cutoff frequencies, harmonic resonances are attenuated, while maintaining in-band performances. In addition, transmission losses may be reduced as the insertion technique leads to optimum designs in terms of overall size. The approach described here is based upon the combination of classical synthesis techniques and optimization procedures provided by conventional computer-aided-design tools. Experimental results are obtained in the case of $\lambda_g/4$ shunt-stub filters implemented in classical semilumped low-pass architectures. Then, we investigate alternative integration technologies and techniques to improve the out-of-band rejection over very wide operating bandwidth. To overcome some design limitations, i.e., workable characteristic impedance value, we propose and validate a multilayer solution. Finally, new low-pass topologies are suggested to improve low-pass filter band rejection.

Index Terms—Bandpass filter, distributed planar filter, low-pass filter, microstrip and multilayer technologies, spurious resonances, synthesis techniques.

I. INTRODUCTION

THE expansion of new telecommunication systems has brought severe constraints and particular requirements for RF front-ends, especially RF filters. Electrical performances regarding either out-of-band rejection or in-band transmission losses have to be considered as well as cost, reliability, or dimensions.

With future multistandard equipments (GSM–DCS–UMTS, Bluetooth), specific needs are also expressed about possible interferences between adjacent operating channels or frequencies. Consequently, RF filters must be used to reduce as much as possible out-of-band spurious harmonics that can be generated by nearby systems or by internal nonlinear front-end functions (power amplifier, mixer, etc.).

At microwave or millimeter-wave frequencies, distributed filters are usually preferred rather than lumped topologies.

Unfortunately, this solution produces unwanted passband regions centered at upper harmonic frequencies (Fig. 1).

This comes from the synthesis procedure based on the equivalence between the ideal electrical scheme, which depends on the selected mathematical transfer function, and corresponding design topologies (resonators, inverters). Since the identification between slope parameters is performed at a center frequency F_0 ,

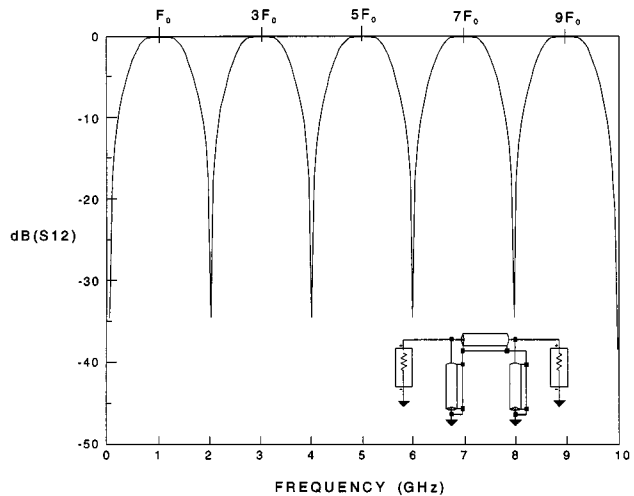


Fig. 1. Broad-band frequency response of a second-order shunt-stub filter with 30% relative bandwidth at 1-GHz center frequency.

unwanted responses, i.e., uncontrolled poles and zeros, occur from constructive combinations at all harmonic orders (Fig. 1).

To attenuate these unwanted responses, a low-pass filter is generally cascaded with the bandpass filter. As a result, both the size of the complete filter and the corresponding transmission losses are increased. In addition, such a technique is only efficient in suppressing the first unwanted bandpass region. The reason is that the same synthesis limitations are encountered for the low-pass filter in terms of unwanted harmonics. Other methods have been proposed such as stepped impedance resonators (SIRs) [1], lumped capacitance insertion [2], and attenuation pole insertion [3].

In this paper, we propose an integration of low-pass filtering structures inside conventional bandpass topologies. Thus, no degradation is expected in terms of insertion losses since the size of the complete filter is not affected. This new configuration requires some specific synthesis effort to define and control the cutoff frequencies of the low-pass elements associated with each bandpass filter section.

Here, the technique is applied to the well-known $\lambda_g/4$ shunt-stub filter [4], but it can be easily extended to other distributed topologies [5]–[7]. This choice is dictated by its design flexibility (well-established synthesis formulas) and technological sensitivity. Also, it appears as the most representative bandpass filter topology regarding the problem of harmonic resonances. First of all, we discuss the efficiency of the insertion technique when considering basic semilumped low-pass sections. The design principle is validated through experimental investigations. However, some discrepancies remain critical due to technological limitations. Original

The authors are with the Laboratoire d'Electronique et Systèmes de Télécommunications, Université de Brest and Ecole Nationale Supérieure des Télécommunications de Bretagne, BP 809-29285 Brest, France.

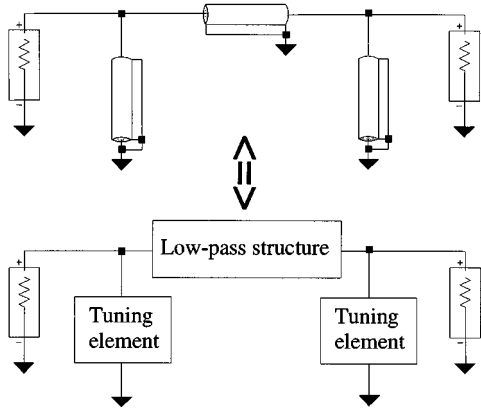


Fig. 2. Insertion of both a low-pass filter within the inverter and tuning elements within resonators.

methods are hence described to overcome these limitations. We first improve the electrical response of the inserted low-pass semilumped topologies in the attenuated band by extending the available characteristic impedance range through an appropriate technological approach [8]–[11]. Finally, we present a new low-pass filter topology [12], [13].

II. METHODOLOGY

The basic distributed bandpass filter topology must be transformed in order to integrate the N th-order low-pass filtering sections. These will contribute to the out-of-band rejection. Depending on the number of parameters, this structural modification leads to very complex equations for which analytical methods are not appropriate. Before implementing an optimization procedure, it is advised to make a preliminary analysis separately on inverters and resonators. In this part, we give details about the transformation made on the inverters, which are considered as low-pass sections, and on the resonators which become tuning elements (Fig. 2).

A. Insertion of Low-Pass Filters Within Series Inverters

A low-pass filter is based upon cascaded inductive and capacitive elements. For a given order N , an inverter is therefore divided into several inductive and capacitive sections. The length of these sections, as well as their corresponding characteristic impedance levels, defines the cutoff frequency of the modified inverter and the out-of-band response.

Inserted low-pass structures have to be synthesized by taking into account various fundamental considerations.

- The achievable inductive and capacitive impedance values mainly affect the out-of-band rejection, depending on the width modifications between cascaded transmission lines and associated parasitic effects. These values depend on the considered technology. For such geometrical discontinuities, a limit width ratio between inductive and capacitive sections must be chosen in accordance with the validity domain of the classical circuit models employed.
- The characteristic impedance of the initial transformer (nonmodified inverter) is now considered as the reference impedance of the low-pass filter. This is a fundamental condition for minimizing the influence of the inserted

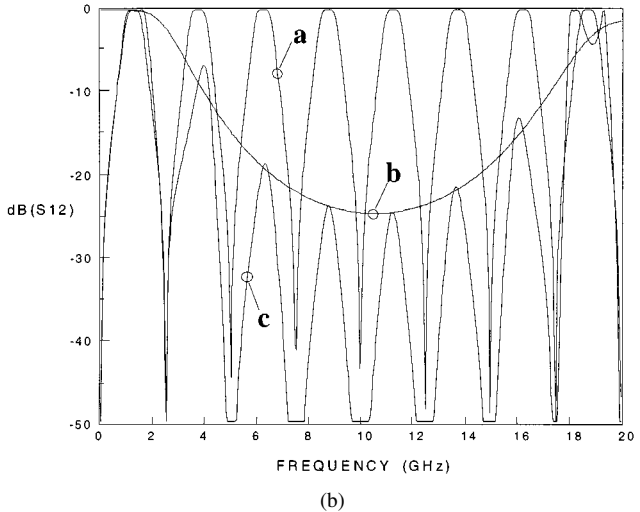
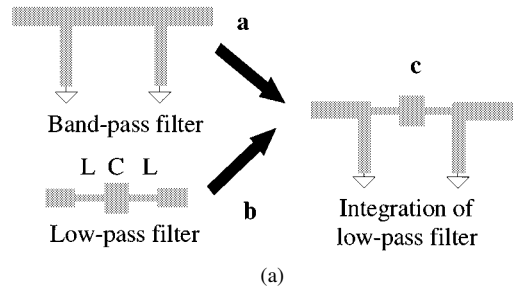


Fig. 3. Illustration of the low-pass filter insertion. (a) Integration of semilumped low-pass filter within the inverter of the bandpass filter. (b) Theoretical associated responses.

low-pass function with respect to the desired operating bandwidth of the bandpass filter.

- The inverter length is close to $\lambda_g/4$ at F_0 (in-band requirements). This parameter is considered, at first, to define the low-pass filter order, i.e., the number N of inductive and capacitive sections. Once N has been selected, the designer can choose the cutoff frequency which is fundamentally related to the length of each capacitive and inductive lines.

Thus, its cutoff frequency cannot be located as close to the operating bandwidth as usually expected. This is illustrated in Fig. 3 where a third-order low-pass structure has been inserted in the center inverter of a second-order bandpass filter. Nevertheless, one can observe some significant improvement of the out-of-band responses due to harmonic rejection.

B. Insertion of Low-Pass Filters Within Parallel Resonators

The same methodology can be considered for integrating filtering structures within parallel $\lambda_g/4$ resonators. However, the degradation of the out-of-band response of the bandpass filter is not really related to the modified parallel resonator. In fact, discrete parasitic recombination nearby operating bandwidth (parasitic constructive response) due to the parallel and series element interaction may occur. To avoid this, the resonator shape can be optimized for ensuring a perfect synchronization. This is done by recovering proper phase conditions with respect to the inverter response. As a result, the modified resonators are considered as tuning elements rather than filtering structures. They

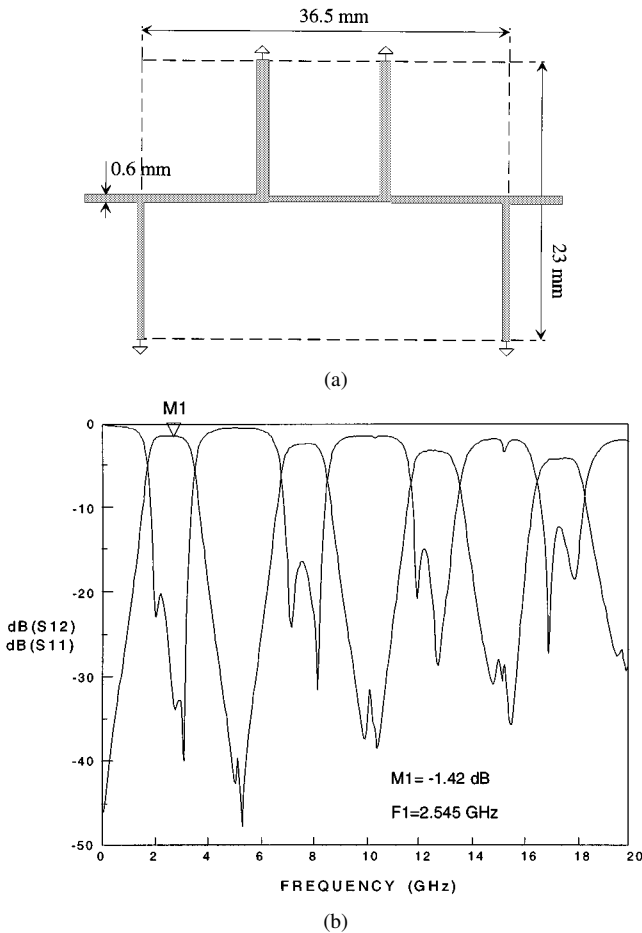


Fig. 4. Classical microstrip shunt-stub filter. (a) Layout. (b) Experimental response.

are therefore synthesized during the final procedure calculation of the complete filter, where series low-pass filter cutoff-frequency and parallel resonator transmission zero values are optimized. This optimization task is easily carried out, by using standard numerical procedure available on commercial computer-aided design (CAD) software.

III. ILLUSTRATIVE EXAMPLES: MODIFIED MICROSTRIP FILTERS

Experimental investigations were carried out in order to validate the concept of such modified filters in microstrip technology. A $635\text{-}\mu\text{m}$ -thick substrate with $\epsilon_r = 10.2$ was used. A fourth-order bandpass filter centered at 2.5 GHz with a relative bandwidth of 40% was designed. Fig. 4 presents the measured response, which corresponds to a nonmodified structure, and the equivalent layout.

As expected, spurious resonances are observed at harmonic frequencies with respect to F_0 . The modified architectures are reported in Figs. 5 and 6 for $L-C-L$ and $C-L-C$ low-pass filters segmentation, respectively.

A $100\text{-}\mu\text{m}$ microstrip line width was used to synthesize inductive sections ($Z_L = 95 \Omega$). The $25\text{-}\Omega$ characteristic impedances corresponding to capacitive sections are implemented through 2-mm strip widths (Fig. 7). Such dimensions were chosen in order to use step discontinuities properly defined by usual transmission-line models, available on commercial CAD software.

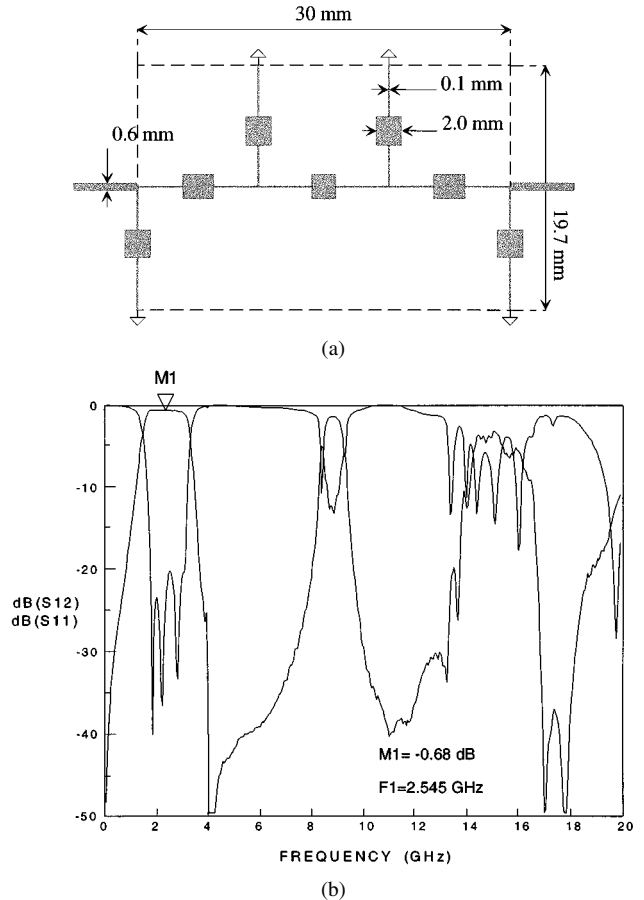


Fig. 5. Modified ($L-C-L$) microstrip shunt-stub filter. (a) Layout. (b) Experimental response.

One should note that the insertion technique contributes to reduce the overall size and the transmission losses. As illustrated in Figs. 4–6, modified topologies both yield quite good results; the first harmonic is well rejected with minor degradations in the operating bandwidth. Measurements performed on the conventional and the modified $L-C-L$ and $C-L-C$ filters yield transmission losses of 1.42, 0.68, and 0.99 dB, respectively. However, the $L-C-L$ version provides better performances near the first harmonic frequency. Indeed, the physical decomposition of the resonators and inverters in $L-C-L$ or $C-L-C$ topologies defines the effective location of corresponding transmission zero.

Then, we have shown that the low-pass filter insertion technique gives quite good results regarding out-of-band rejection while maintaining the in-band behavior. However, only the first spurious resonance is suppressed due to the reduced selectivity of low-pass structures and the difficulty for the designer to define optimal cutoff frequencies. This is due to the strong influence of the fundamental filter elements which impose specific constraints on dimensions and design flexibility.

We propose two alternate solutions for overcoming these limitations:

- 1) multilayer integration approach to obtain a wider range of characteristic impedance values;
- 2) original low-pass filter topologies to replace the usual semilumped ones and, therefore, improve the out-of-band rejection.

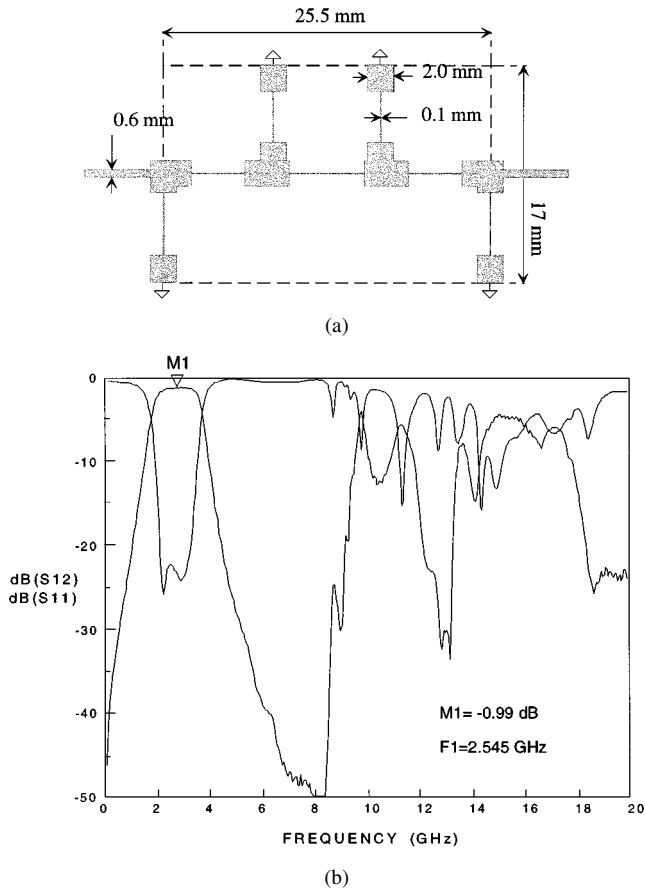


Fig. 6. Modified (C-L-C) microstrip shunt-stub filter. (a) Layout. (b) Experimental response.

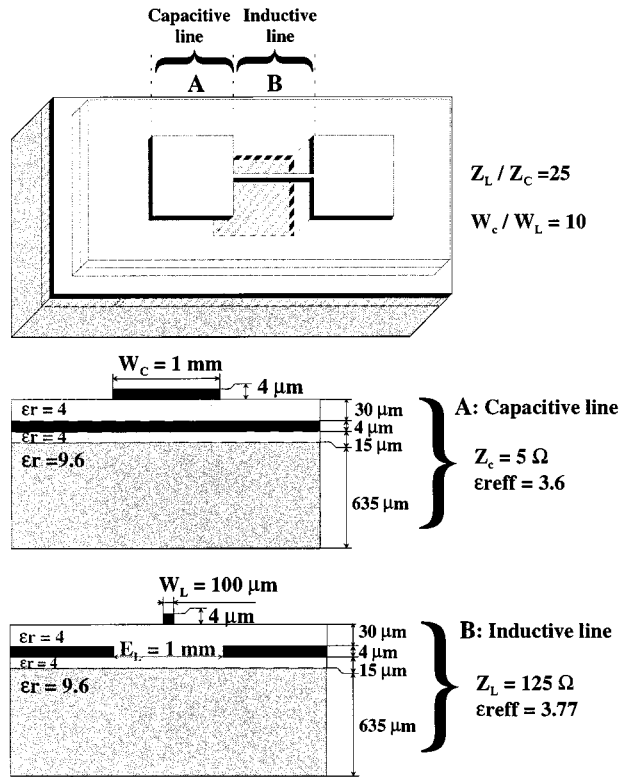


Fig. 8. Design of inductive and capacitive lines in multilayer technology.

IV. MULTILAYER TECHNOLOGY IMPLEMENTATION

A. Presentation of the Technology

The electrical performances of inserted low-pass structures mainly depend on the achievable characteristic impedance range. The higher and lower the values of characteristic impedances for inductive and capacitive sections, respectively, are, the better the out-of band rejection level will be. However, such conditions are met only in the case of convenient step discontinuities between cascaded lumped inductances and capacitances. Thus, appropriate technologies must be used to achieve such impedance values.

Multilayer integration techniques appear to be quite attractive. Indeed, the designer can optimize the design by using the numerous overlapping possibilities that not only minimize discontinuity effects, but also provide very low or very high characteristic impedance values.

We investigated a multilayer technology based upon a thick-film technological process. An alumina motherboard substrate ($\epsilon_r = 9.6$ and $h = 635 \mu\text{m}$) was used with additional thin dielectric layers (15 to $20 \mu\text{m}$) of permittivity $\epsilon_r = 4$ alternated with conductive gold layers. Fig. 8 describes two basic technological configurations for both capacitive and inductive multilayer lines.

- In case A, a gold ground plane is deposited on the alumina substrate; the dielectric overlay acts as a thin substrate on which very low characteristic impedance values can be synthesized. This transmission line configuration is named the thin-film microstrip line (TFMS) structure.

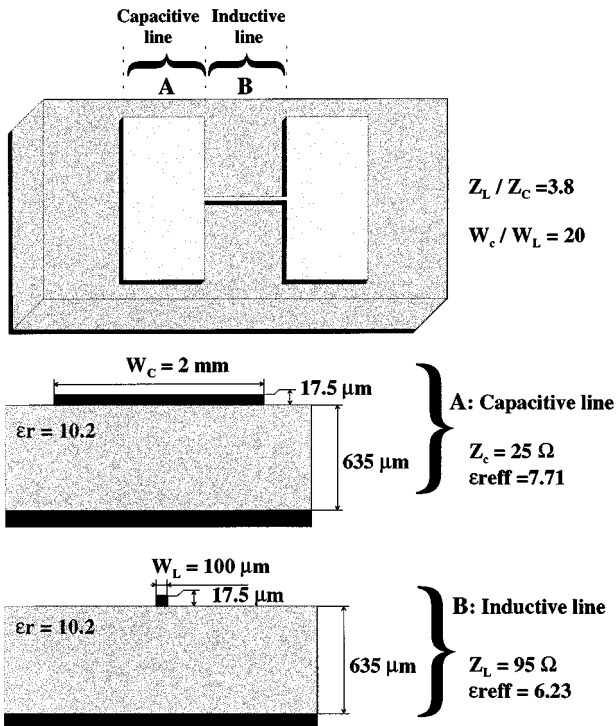


Fig. 7. Design of inductive and capacitive lines in microstrip technology.

- In case B, the previous ground plane can be locally suppressed to obtain quite high impedance values. Intermediate insulating dielectric layers may be placed between the ground plane and the alumina motherboard. This results in a significant increase of the transmission line characteristic impedance values which can be assumed as a three-dimensional (3-D) coplanar waveguide. Consequently, the great flexibility associated to the design of coplanar transmission lines is also valid for such 3-D configuration.

Figs. 7 and 8 compare the capacitive and inductive lines available with each approach. For similar center conductor dimensions, 95- and 125- Ω characteristic impedances can be achieved with the microstrip and multilayer technologies, respectively. Low characteristic impedance values of 25 and 5 Ω are obtain with microstrip and multilayer technology, respectively. In this last case, the conductor width is smaller. In conclusion, with the multilayer approach, a Z_L -to- Z_C impedance ratio between inductive and capacitive elements is improved by a factor of seven while the corresponding W_C -to- W_L width ratio is divided by a factor of two. The impedance ratio is, therefore, significantly increased, which greatly improves the out-of-band responses of semilumped low-pass filters. The above geometric values bring the advantage to allow the use of standard CAD models, thus avoiding full-wave analysis.

B. Examples of Design

A second-order bandpass filter including low-pass filters was designed by using this multilayer technology. As reported in Fig. 9, input-output coplanar access is used for on-wafer measurements and via-to-ground connections are made for shunt-stubs.

The filter was designed at 2.6 GHz with a relative bandwidth of 16%. Measurements were made on a wide operating bandwidth from 0 to 40 GHz. Fig. 9 shows quite a high attenuation level of spurious resonances up to the eleventh harmonic (22 GHz). In addition, the in-band performances are, moreover, preserved with a return loss of about -14 dB and insertion losses of -1.1 dB.

The same procedure was tested for another geometrical ratio between inductive and capacitive transmission lines that constitute the inserted low-pass filters. For a width ratio decreased to 5 ($Z_C = 10 \Omega$ and $Z_L = 120 \Omega$), experimental results remain almost identical to the previous ones (Fig. 10). The first spurious resonance is rejected up to the eighth harmonic with respect to the center frequency.

V. SYNTHESIS OF EFFICIENT LOW-PASS FILTERS

More efficient synthesis techniques can also be developed to improve the out-of-band response of low-pass filters. We have already considered the well-known semilumped synthesis which, unfortunately, leads to bad performances as shown at high frequencies. Alternate multilayer integration techniques can be employed, but may become costly and, hence, are not really well-suited for mass production.

We propose to synthesize new topologies of low-pass filters based upon a combination of semilumped and distributed structures (open stubs as parallel capacitance, and admittance inverters as series inductances). This original combination can

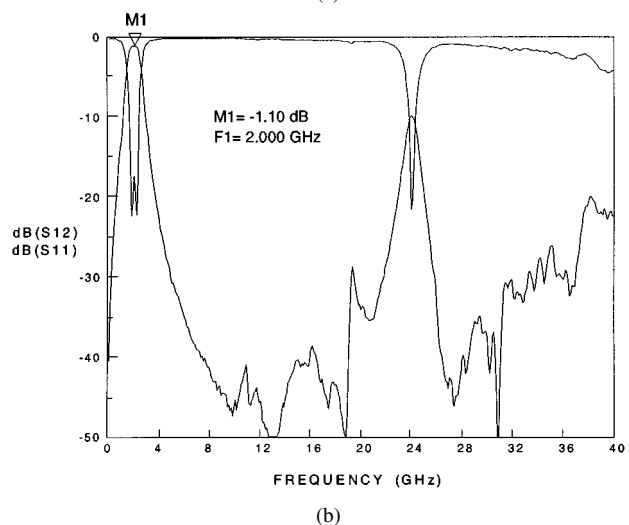
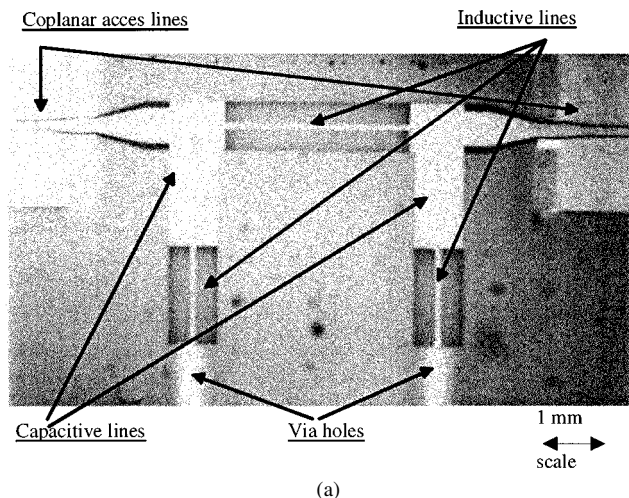


Fig. 9. Modified second-order multilayer shunt-stub filter. (a) Photograph. (b) Experimental response.

take advantage of the properties related to each basic element:

- open stubs give a high rejection level near the operating bandwidth;
- impedance inverters can be compared to semilumped inductance (Fig. 11).

Using the chain matrix of each element, direct identifications can be written between the L and C values of the ideal low-pass filter scheme and the corresponding transmission-line characteristics.

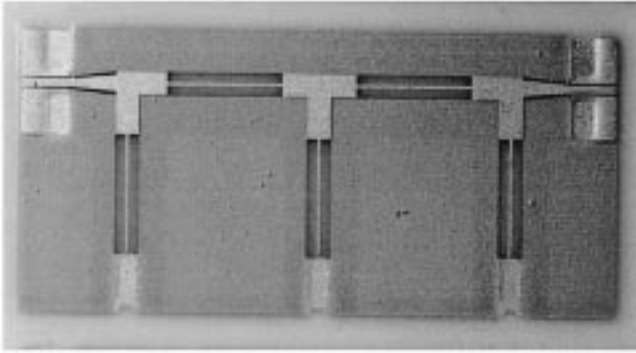
We change the usual synthesis formulas by artificially modifying the effective electrical length of the capacitive and inductive sections. “ a ” and “ b ” coefficients can be adjusted to obtain workable characteristic impedance values Z_C and Z_L given by

$$Z_C = \tan\left(\frac{bw_C l_C}{c}\right) / C w_C \quad (1)$$

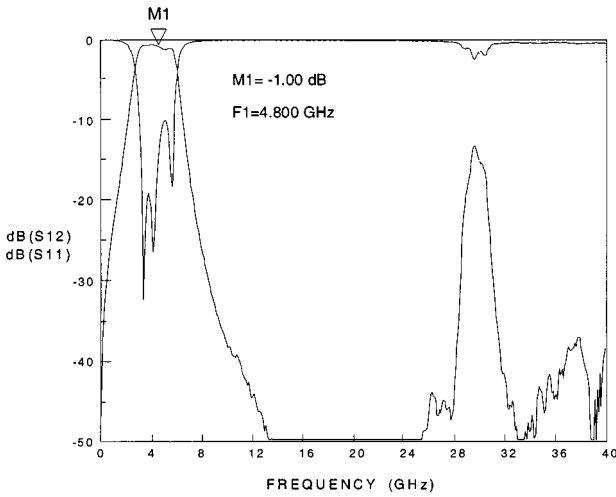
$$Z_L = L w_C / \sin\left(\frac{aw_C l_C}{c}\right) \quad (2)$$

with
 ω_C
 c
 l_C

cutoff pulsation;
 speed of light in vacuum;
 initial length of lines.



(a)



(b)

Fig. 10. Modified third-order multilayer shunt-stub filter. (a) Photograph. (b) Experimental response.

Thus, “ a ” and “ b ” artificially modify the electrical length of stubs and inverters. This results in a new set of characteristic impedances. The designer has, then, the opportunity to control and use achievable values for Z_C and Z_L while taking into account the intrinsic limitations of the selected technology.

We investigate a new calculation procedure which is depicted in Fig. 12. The values of a and b are chosen at once in accordance with the technological possibilities.

We have determined various configurations for a and b corresponding to particular situations.

If $a < b$, the resonances induced by the inductive line occur at frequencies greater than the ones produced by the stubs. In this case, the synthesis limitations are related to the lowest Z_C achievable value.

If $b < a < 2b$, in this case, the undesired resonance of the central line takes place between the filter cutoff frequency and the first parasitic resonance of the stubs. Consequently, we consider $a = 2b$ in order to synchronize this resonance with the stub’s transmission zero localization.

If $a > 2b$, additional resonance is encountered and the out-of-band control become impossible. A specific algorithm procedure has been implemented taking into account the lowest and highest characteristic impedance Z_{MIN} and Z_{MAX} achievable with the selected technology.

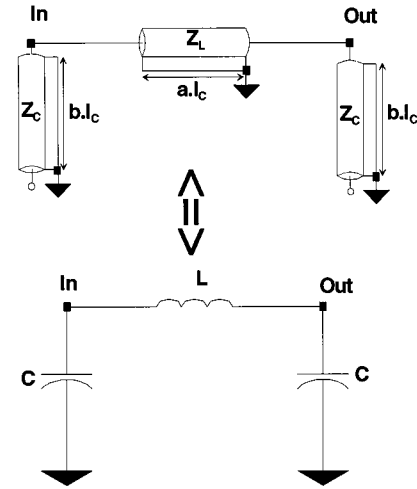


Fig. 11. Identification between ideal and semilumped schemes.

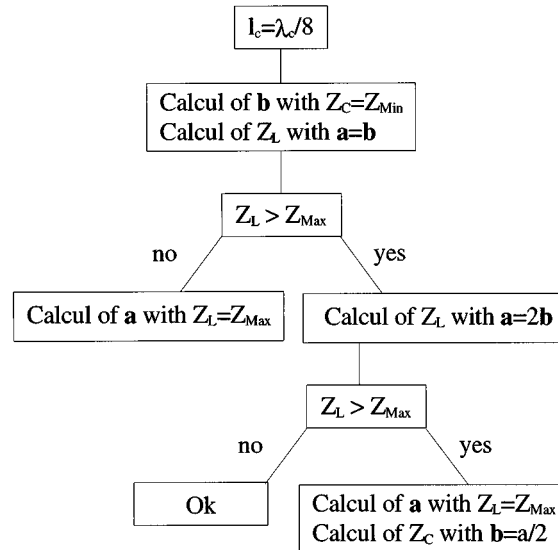


Fig. 12. Procedure of calculation.

Fig. 13 displays a comparison between semilumped and modified low-pass filters. The high frequency rejection level is significantly improved despite the use of standard characteristic impedance values. Therefore, one can use the design flexibility brought by additional variables “ a ” and “ b ” to obtain convenient Z_C and Z_L values, and thus improve the out-of-band response.

Fig. 14 presents a third-order microstrip low-pass filter made with modified synthesized structures. A 635- μm -thick substrate, with $\epsilon_r = 10.2$ was used. In accordance with the involved technological process and the synthesis procedure, we define the following values for “ a ” and “ b ” tuning parameters: “ a ” = 0.688 and “ b ” = 0.344. Then, Z_C and Z_L are equal to 25 and 85 Ω , respectively. Measurements show the rejection of spurious resonances up to the eighth harmonic ($F_C = 1$ GHz), which is good compared to conventional planar topologies.

Such a basic structure was inserted within the inverters of a bandpass filter; it included input–output electrical length for recovering the phase conditions (which corresponds to the inverter effects) and minimizing parasitic coupling between adjacent capacitive stubs and parallel shunt resonators. Good performances

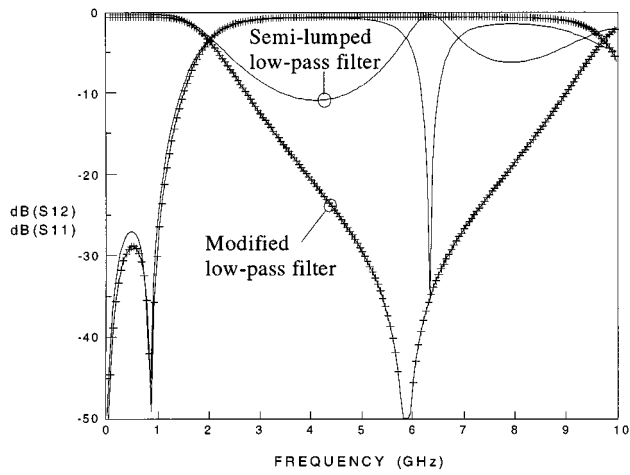


Fig. 13. Theoretical responses: comparison between the semilumped low-pass and modified low-pass filters (microstrip technology with workable characteristic impedance values).

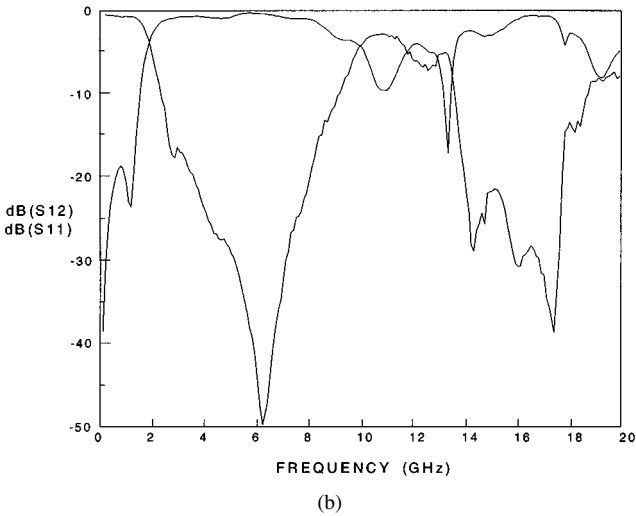
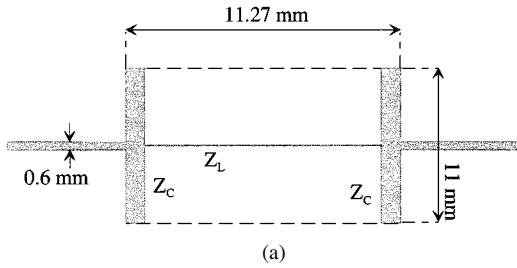


Fig. 14. Modified microstrip low-pass filter. (a) Layout. (b) Experimental response.

were obtained (a return loss better than 25 dB and insertion losses below 1.1 dB), with rejection of spurious resonance up to the sixth harmonic (6 GHz) (Fig. 15).

A dual low-pass filter topology can be also used ($L-C-L$ topology): it allows one to obtain a stronger decoupling effect between adjacent structures. The results brought by both original integration techniques are interesting in terms of losses and rejection level. In addition, the dimensions are not increased and the technological reliability is maintained (Fig. 16).

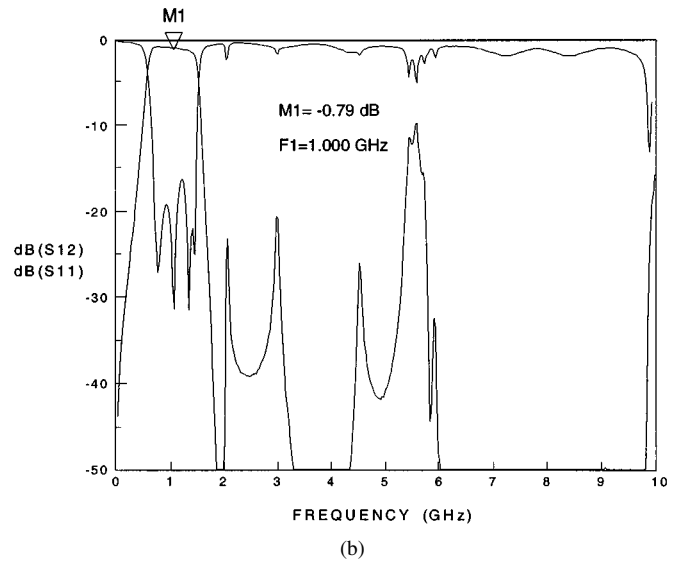
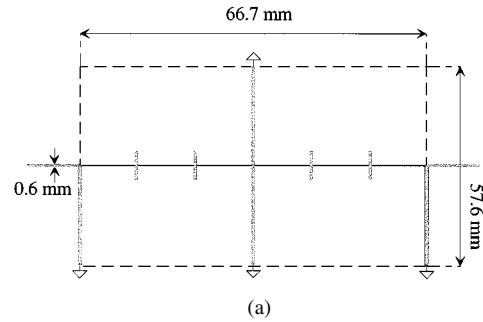


Fig. 15. Modified ($C-L-C$) microstrip shunt-stub filter. (a) Layout. (b) Experimental response.

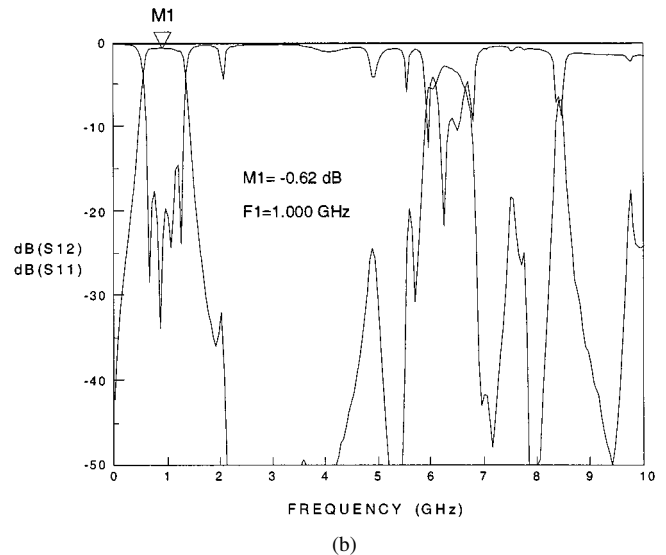
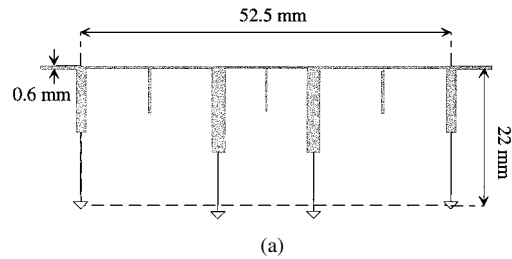


Fig. 16. Modified ($L-C-L$) microstrip shunt-stub filter. (a) Layout. (b) Experimental response.

VI. CONCLUSION

This paper describes original approaches related to the improvement of bandpass filter performances. The insertion of low-pass filters into conventional resonant structures appears as a convenient solution to suppress spurious responses in a desired rejected bandwidth, without increasing the overall size and insertion losses.

First, we considered classical bandpass filters and analyzed in detail the problems induced by direct integration or association of bandpass and low-pass structures.

Then, design rules were validated through theoretical and experimental comparisons. The main limitations in relation to the integration technique were discussed. Then, two original solutions for overcoming these limitations were proposed. These investigations led us to develop improved multilayer integration techniques as well as original low-pass synthesis topologies.

The integration concept proposed here is easily applicable to other types of structures and functions. For example, in the future we intend to apply the insertion method to wide-band couplers commonly used in distributed balanced mixers. Indeed, couplers with inserted low-pass arms could control the matching conditions not only at the fundamental frequencies F_{OL} , F_{RF} or F_{FI} , but also at any other harmonic generated by the mixing Schottky diodes. This would significantly reduce the conversion losses.

Current work concerns the improvement of the integration concept performances by considering the implementation of the new low-pass filter topology with 3-D technology [14].

REFERENCES

- [1] S. Denis, C. Person, S. Toutain, S. Vigneron, and B. Theron, "Improvement of global performances of band-pass filters using nonconventional stepped impedance resonators," in *EuMC*, vol. 2, Amsterdam, The Netherlands, October 5–7, 1998, p. 323.
- [2] Y. Noguschi and J. Ishii, "New compact bandpass filters using lambda coplanar waveguide resonators and method for suppressing these spurious responses," *Electron. Commun.*, vol. 77, no. 3, pp. 66–73, 1994.
- [3] M. Tsuji and H. Shigesawa, "Spurious response suppression in broadband and introduction of attenuation poles as guard bands in printed-circuit filters," in *EuMC*, vol. 3, Paris, France, Oct. 2–5, 2000, p. 44.
- [4] G. Matthaei, L. Young, and E. M. T. Jones, *Microwave Filters, Impedance-Matching Networks, and Coupling Structures*. Norwood, MA: Artech House, 1980, pp. 594–598.
- [5] U. Karacaoglu, D. Sanchez-Hernandez, I. D. Robertson, and M. Guglielmi, "Harmonic suppression in microstrip dual-mode ring-resonator bandpass filters," in *IEEE MTT-S Int. Microwave Symp. Dig.*, San Francisco, CA, June 1996, pp. 1635–1638.
- [6] J. Marti and A. Griol, "Harmonic suppressed microstrip multistage coupled ring bandpass filters," *Electron. Lett.*, vol. 34, no. 2, pp. 2140–2142, Oct. 1998.
- [7] E. Rius, J. Ph. Coupez, A. Perennec, G. Tanne, and S. Toutain, "Integration of low-pass structures in band-pass structures. Application to the control of spurious resonance," in *EuMC*, vol. 2, Amsterdam, The Netherlands, October 5–7, 1998, p. 44.
- [8] W. Schwab, F. Boegelsack, and W. Menzel, "Multilayer suspended stripline and coplanar line filters," *IEEE Trans. Microwave Theory Tech.*, vol. 42, pp. 1404–1407, July 1994.
- [9] C. Person, L. Carre, E. Rius, S. Toutain, and J. Ph. Coupez, "Original techniques for designing wideband 3D integrated couplers," in *IEEE MTT-S Int. Microwave Symp. Dig.*, vol. 1, Baltimore, MD, June 1998, pp. 119–122.
- [10] M. Gillick and I. D. Robertson, "Ultra low impedance CPW transmission lines for multilayer MMICs," in *IEEE MTT-S Int. Microwave Symp. Dig.*, Atlanta, GA, June 1993, pp. 145–148.

- [11] C. Quendo, J. Ph. Coupez, C. Person, E. Rius, M. Le Roy, and S. Toutain, "Band-pass filters with self-filtering resonators: A solution to control spurious resonances," in *IEEE MTT-S Int. Microwave Symp. Dig.*, vol. 3, Anaheim, CA, June 1999, pp. 1135–1138.
- [12] D. M. Pozar, *Microwave Engineering*. Reading, MA: Addison-Wesley, 1993, pp. 498–500.
- [13] C. Quendo, C. Person, E. Rius, and M. Ney, "Optimal design of low-pass filters using open stubs to control out-of-band," in *EuMC*, vol. 3, Paris, France, Oct. 2–5, 2000, p. 338.
- [14] D. Ahn, J.-S. Park, C.-S. Kim, J. Kim, Y. Qian, and T. Itoh, "A design of the low-pass filter using the novel defected ground structure," *IEEE Microwave Theory Tech.*, vol. 49, pp. 86–92, Jan. 2001.